

## RESEARCH ARTICLE

# Combined electrophysiological and morphological phenotypes in patients with genetic generalized epilepsy and their healthy siblings

Christina Stier<sup>1,2</sup>  | Markus Loose<sup>1</sup> | Raviteja Kotikalapudi<sup>1,2,3</sup> |  
 Adham Elshahabi<sup>2,4</sup> | Yiwen Li Hegner<sup>2</sup> | Justus Marquetand<sup>2,5</sup> |  
 Christoph Braun<sup>2,6,7</sup> | Holger Lerche<sup>2</sup> | Niels K. Focke<sup>1,2</sup> 

<sup>1</sup>Clinic of Neurology, University Medical Center Göttingen, Göttingen, Germany

<sup>2</sup>Department of Neurology and Epileptology, Hertie Institute for Clinical Brain Research, University of Tübingen, Tübingen, Germany

<sup>3</sup>Institute of Psychology, University of Bern, Bern, Switzerland

<sup>4</sup>Department of Neurology, University Hospital Zurich, Zurich, Switzerland

<sup>5</sup>Department of Neural Dynamics and Magnetoencephalography, Hertie Institute for Clinical Brain Research, University of Tübingen, Tübingen, Germany

<sup>6</sup>Magnetoencephalography Center, University of Tübingen, Tübingen, Germany

<sup>7</sup>Center for Mind/Brain Sciences, University of Trento, Rovereto, Italy

## Correspondence

Niels K. Focke and Christina Stier, Universitätsmedizin Göttingen, Klinik für Neurologie, Robert-Koch-Str 40, 37075 Göttingen, Germany.

Email: [niels.focke@med.uni-goettingen.de](mailto:niels.focke@med.uni-goettingen.de)

and [christina.stier@med.uni-goettingen.de](mailto:christina.stier@med.uni-goettingen.de)

## Funding information

Deutsche Forschungsgemeinschaft, Grant/Award Number: FO 750/5-1

## Abstract

**Objective:** Genetic generalized epilepsy (GGE) is characterized by aberrant neuronal dynamics and subtle structural alterations. We evaluated whether a combination of magnetic and electrical neuronal signals and cortical thickness would provide complementary information about network pathology in GGE. We also investigated whether these imaging phenotypes were present in healthy siblings of the patients to test for genetic influence.

**Methods:** In this cross-sectional study, we analyzed 5 min of resting state data acquired using electroencephalography (EEG) and magnetoencephalography (MEG) in patients, their siblings, and controls, matched for age and sex. We computed source-reconstructed power and connectivity in six frequency bands (1–40 Hz) and cortical thickness (derived from magnetic resonance imaging). Group differences were assessed using permutation analysis of linear models for each modality separately and jointly for all modalities using a nonparametric combination.

**Results:** Patients with GGE ( $n = 23$ ) had higher power than controls ( $n = 35$ ) in all frequencies, with a more posterior focus in MEG than EEG. Connectivity was also increased, particularly in frontotemporal and central regions in theta (strongest in EEG) and low beta frequencies (strongest in MEG), which was eminent in the joint EEG/MEG analysis. EEG showed weaker connectivity differences in higher frequencies, possibly related to drug effects. The inclusion of cortical thickness reinforced group differences in connectivity and power. Siblings ( $n = 18$ ) had functional and structural patterns intermediate between those of patients and controls.

**Significance:** EEG detected increased connectivity and power in GGE similar to MEG, but with different spectral sensitivity, highlighting the importance of theta and beta oscillations. Cortical thickness reductions in GGE corresponded to

functional imaging patterns. Our multimodal approach extends the understanding of the resting state in GGE and points to genetic underpinnings of the imaging markers studied, providing new insights into the causes and consequences of epilepsy.

#### KEYWORDS

cortical thickness, endophenotypes, interictal, oscillations, resting state

## 1 | INTRODUCTION

Genetic generalized epilepsy (GGE) is a common epilepsy syndrome with polygenic etiology.<sup>1</sup> Rapid neuronal changes such as generalized spike-wave discharges (GSWD) or generalized seizures are a hallmark of GGE. However, the link between the genetic pathology underlying the disease and its systemic effects on macroscale brain dynamics is not well understood. Using magnetoencephalography (MEG), we have previously shown that increased resting state power and network synchronization are characteristic of GGE and are similarly present in healthy siblings of the patients.<sup>2</sup> We hypothesized that this could also be observed with electroencephalography (EEG), which is generally more available than MEG as a diagnostic tool in routine clinical practice. In principle, MEG and EEG signals reflect the same neuronal sources. However, due to the different sensitivity profiles of the techniques, one can expect that the recording of both signals could also reveal complementary information.<sup>3</sup> For GGE, few studies have exploited the benefit of employing both EEG and MEG together, and most have focused on localizing the source of GSWD.<sup>4,5</sup> Using both techniques in the same individuals at rest could therefore provide additional information about aberrant networks in GGE that are central to the classification of the disease. In addition to functional alterations in GGE, subtle structural changes such as cortical thinning are known.<sup>6</sup> However, the relationship between those changes and fast oscillatory neuronal activity in GGE has not been investigated in detail. Atrophic patterns could result from disease progression or disease activity,<sup>7</sup> but the evidence is inconclusive,<sup>8</sup> and longitudinal studies are lacking. Cortical thickness reflects cell density and cytoarchitecture, among other factors, and is highly heritable.<sup>9</sup> Consequently, microstructural changes in GGE may be genetically driven and linked to electrophysiological alterations. If so, the statistical combination of all three modalities, that is, EEG, MEG, and magnetic resonance imaging (MRI) in the same cohort, should point to common network alterations. Together with attempts to understand the heritability of these states,

#### Key Points

- Interictal states in GGE were characterized by widespread increases in fast oscillatory activity and synchronization
- Network conditions were similarly detected by EEG and MEG, but with spectral and spatial differences
- GGE network changes were reflected in the broadband, but particularly in theta and beta frequencies
- Cortical thinning in GGE was related to functional patterns and amplified group contrasts
- Similar structural and functional phenotypes in healthy siblings suggest a genetic influence

this could lead to improved diagnosis and prognosis for GGE in the future. GGE markers that are heritable, so-called endophenotypes,<sup>10</sup> are thought to reflect causative disease mechanisms rather than clinical presentation. Some functional and structural MRI research has demonstrated such traits of GGE subtypes,<sup>7,11–15</sup> including increased activations of the motor system,<sup>12–15</sup> aberrant cortical folding and surface,<sup>7</sup> and abnormal hippocampal structure and function.<sup>11</sup> So far, there is little evidence of such endophenotypic markers at higher temporal resolution<sup>16</sup> and in mixed GGE types.

Here, we adopted a multimodal approach that integrated structural and functional features of GGE to promote a more holistic understanding of GGE network pathology and its genetic basis. In a first step, we compared EEG to MEG resting state measurements in a subset of a previously reported study cohort,<sup>2</sup> focusing on EEG results in detail. We then integrated both modalities in a unified statistical analysis and explored the correspondence between cortical thickness and functional group maps. Finally, we examined whether the functional and structural changes could be genetically determined by studying healthy siblings of the patients.

## 2 | MATERIALS AND METHODS

### 2.1 | Participants

We acquired data from 28 patients, 21 healthy siblings, and 50 controls, who were recruited consecutively through the Department of Neurology, University Hospital of Tübingen, Germany, and in the local area. For comparison of EEG and MEG findings and joint inference analysis, we reanalyzed individuals from our previous MEG study,<sup>2</sup> for whom both EEG and MEG recordings were available. After exclusion of data due to technical problems, artifacts, or sleep during recordings, 23 patients, 18 siblings (related to 13 patients), and 35 controls were considered further (two patients and 10 controls fewer than in Stier et al.<sup>2</sup>). The groups were comparable for sex ( $\chi^2 = .5, p = .78$ ) and age ( $F = .1, p = .91$ ; see demographics in Table S1). Siblings and controls were free of any neurologic or psychiatric disorders, had never experienced seizures, and did not take any medication at the time of the measurements. Patients were diagnosed with GGE according to the International League Against Epilepsy.<sup>17</sup> For more clinical details, see Table S2. All MRI scans were visually rated as normal except for three non-specific findings (two patients with uncomplicated cysts and one patient with a nonspecific white matter lesion). Study approval was received from the local ethics committee of the Medical Faculty of the University of Tübingen. The study was conducted in compliance with the principles of the Declaration of Helsinki. All individuals gave informed consent to participate in the study.

### 2.2 | EEG/MEG recordings

The individuals were measured in a supine position at the MEG center of the University of Tübingen, using a 275-channel MEG system (CTF) and subsequently, after a short break, using a 256-channel EEG system (GES400; EGI/Philips-Neuro). We continuously recorded 30 min of resting state data with eyes closed for each subject (sampling rate: EEG, 1 kHz; MEG, 568 Hz) and instructed the individuals to relax, not to fall asleep, and not to think of anything in particular. This rather long acquisition time was chosen to obtain sufficient data after exclusion of segments with GSWD.

### 2.3 | MRI acquisition

All individuals underwent MRI scanning either on a Siemens Magnetom Trio 3-T scanner equipped with a 12-channel head coil (10/35 controls, 4/23 patients)

or on the Siemens Magnetom Prisma 3-T system with a 64-channel head coil (25/35 controls, 18/18 siblings, 19/23 patients). Sagittal high-resolution T1-weighted images were acquired (three-dimensional magnetization-prepared rapid acquisition gradient echo, repetition time = 2.3 s, echo time = 3.03 ms, flip angle = 8°, voxel size = 1 × 1 × 1 mm).

### 2.4 | Surface-based mapping

FreeSurfer 6.0.0 (<https://surfer.nmr.mgh.harvard.edu/>) was used to reconstruct individual cortical surfaces sampled at the pial and the gray–white boundary ("smoothwm"). To ensure anatomical correspondence among individuals and modalities, we applied SUMA<sup>18</sup> to recreate each surface (density factor = 10) based on a FreeSurfer standard template ("fsaverage"). This procedure yielded 1002 common vertices per hemisphere for cortical thickness estimations and as EEG/MEG source points, allowing vertex-based group contrasting.

### 2.5 | EEG/MEG head models

To conduct source-level analyses, we built volume conduction models based on individual cortical meshes yielded by the SUMA procedure and SPM12 (<https://www.fil.ion.ucl.ac.uk/spm/software/spm12/>) brain segmentations. The EEG electrodes were aligned with the anatomical landmarks (nasion, preauricular points) and projected onto the scalp mesh. For MEG, cortical meshes were realigned to the CTF sensor space using fiducial positions marked in the magnetic resonance image and reference coils placed during the measurements. Lead fields were computed based on either a three-layer boundary element model for EEG or a single-shell model for MEG using Fieldtrip<sup>19</sup> in MATLAB (v9.0, R2016a, MathWorks). More technical details and references can be found elsewhere.<sup>20</sup>

### 2.6 | Data processing and source localization

EEG and MEG data were separately processed using Fieldtrip.<sup>19</sup> We applied a first-order Butterworth band-pass filter (1–70 Hz) and a band-stop filter to remove line noise (at 50, 100, and 150 Hz). Data were downsampled (150 Hz) and segmented into trials of 10-s length. Each trial was visually inspected and rejected if noisy (e.g., muscle artifacts, sensor jumps). We also excluded trials with GSWD plus trials preceding and following the event by  $\pm 10$  s. Cardiac artifacts and eye movements were

extracted by independent component analyses and manually rejected. In a second review, we scored vigilance of the individuals according to the criteria of the American Academy of Sleep Medicine (<https://aasm.org/>). Only trials rated as awake were further considered. Thirty trials were randomly selected for source analysis, because previous work has shown good reliability for the metrics of interest for 5 min of data.<sup>20</sup>

Spectral analyses were performed using fast Fourier time-frequency transforms and multitapers for six frequency bands (delta,  $2 \pm 2$  Hz; theta,  $6 \pm 2$  Hz; alpha,  $10 \pm 2$  Hz; beta1,  $16 \pm 4$  Hz; beta2,  $25 \pm 4$  Hz; gamma,  $40 \pm 8$  Hz). Signal power and cross-spectral densities were estimated on the Fourier-transformed sensor data and projected to the source space using beamforming<sup>21</sup> in each frequency band. Power was calculated for each vertex and the coherency coefficient between all pairs of vertices ( $n = 2004$ ). We derived the absolute imaginary part of coherency as our connectivity measure quantifying phase synchrony between signals less affected by potential field spread.<sup>22</sup> To determine the total connectivity for each vertex, we averaged the strength of all its connections. We also computed a global power and connectivity value for each participant by averaging across all vertices.

## 2.7 | Cortical thickness

Cortical thickness quantifies the distance between the gray-white matter and pial boundaries and was computed at each SUMA vertex (FreeSurfer procedure). Thickness maps were smoothed with a heat kernel of size 12 mm full width at half maximum<sup>23</sup> in AFNI (<https://afni.nimh.nih.gov/>) to account for residual spatial differences among individuals.

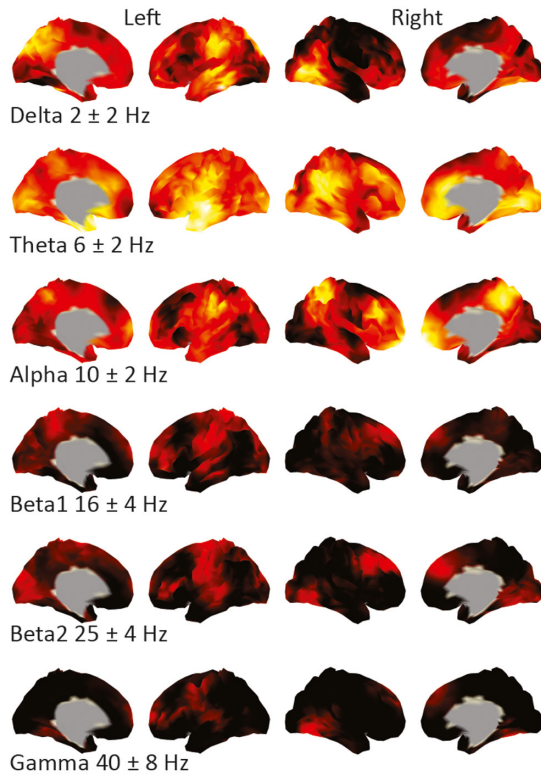
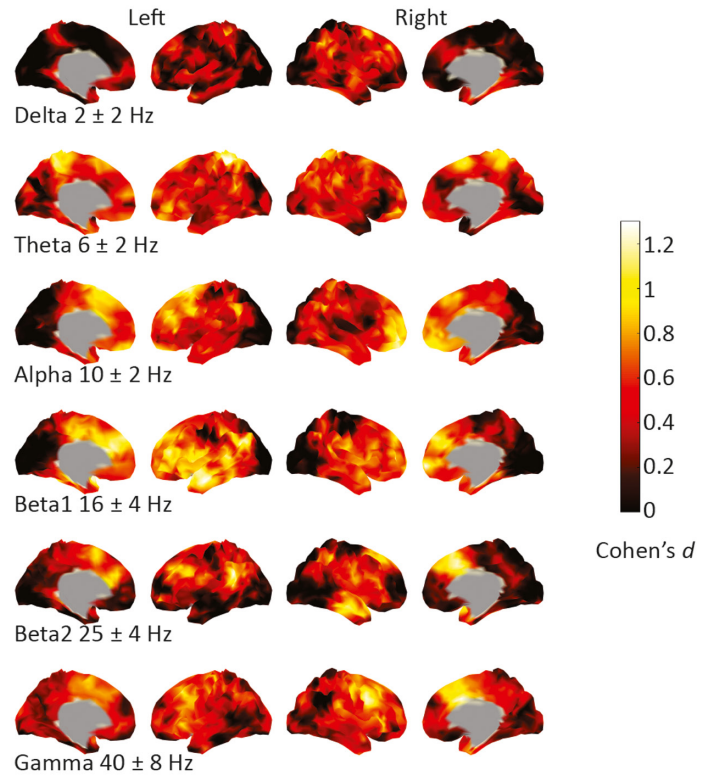
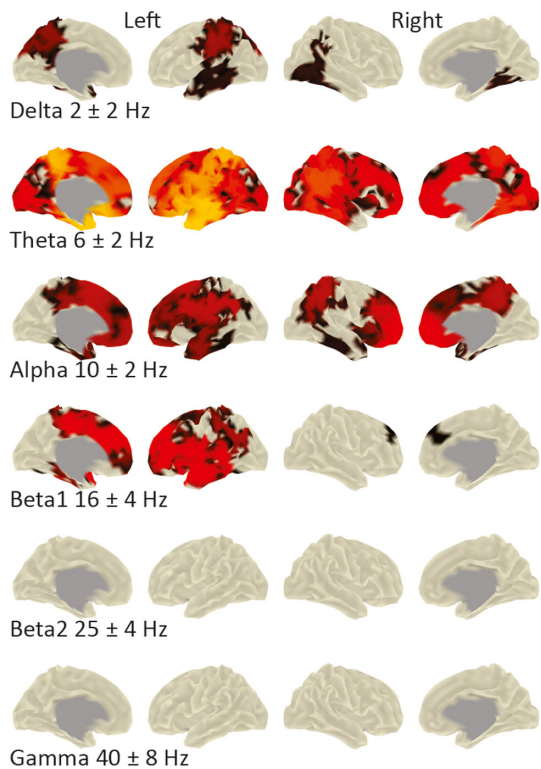
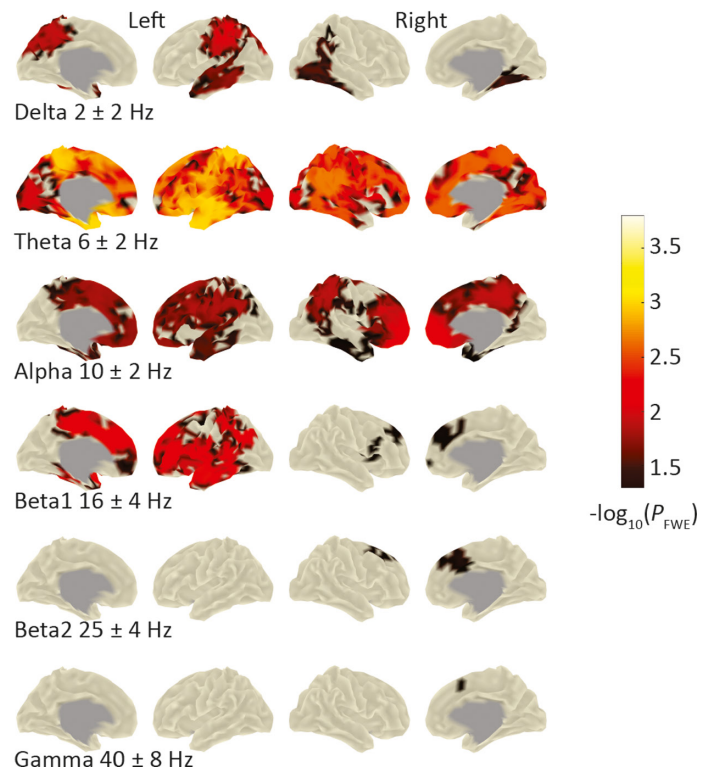
## 2.8 | Joint inference

We performed joint analyses of EEG, MEG, and MRI metrics using nonparametric combination<sup>24</sup> in

Permutation Analysis of Linear Models (PALM), a statistical tool (<https://fsl.fmrib.ox.ac.uk/fsl/fslwiki/PALM>). We hypothesized the existence of increased EEG and MEG connectivity and power as well as reduced cortical thickness in patients compared with controls with corresponding intermediate values in siblings. To obtain concordant directions of the modalities, we multiplied individual cortical thickness values by  $-1$  when combining with functional data. First, one-sided  $t$  contrasts were separately tested for each modality based on synchronous permutations across modalities to account for dependencies. In brief, general linear models were fitted for each vertex individually, and one at the global level, with group, age, sex, total intracranial volume, and scanner site as independent variables and the imaging metric as dependent variable. Second, we applied Fisher's method<sup>25</sup> to combine test statistics of the modalities for each permutation. This process was repeated for the number of permutations ( $n = 500$ , with tail approximation), resulting in separate (partial tests) and combined empirical distributions (joint tests), from which  $p$ -values were derived. We used tail approximation in PALM for accelerated inference and multilevel block permutation to allow sufficient exchangeability of the data, given relatedness among individuals (for details, see Stier et al.<sup>2</sup>). For each test (partial and joint),  $p$ -values were familywise error (FWE) corrected at the level of clusters resulting from threshold-free cluster enhancement<sup>26</sup> and, in the joint analyses, based on the permutation distribution of the extremum statistics across all modalities. FWE correction was also applied over the three modalities (partial tests). We chose a significance level of  $-\log_{10}p = 1.3$  (equivalent to  $p < .05$ ). Cohen  $d$  was calculated based on the  $t$ -values of the group factors of the linear models and is therefore adjusted for age, sex, and intracranial volume effects.  $d$  describes the standardized mean difference of an effect so that  $d \geq .8$  indicates a large,  $d = .5$  a medium, and  $d = .2$  a small effect.<sup>27</sup> To further explore structural alterations, we spatially remapped cortical thickness measures to 68 brain

**FIGURE 1** Effect sizes of electroencephalography (EEG) and magnetoencephalography (MEG) connectivity increases in genetic generalized epilepsy (GGE), and joint inference with and without cortical thickness. (A, B) Standardized effect sizes (Cohen  $d$ ) for increased connectivity in patients with GGE versus controls using EEG and MEG, respectively. Effect sizes were derived from the  $t$ -values of the permutation analyses of linear models.  $d$  is therefore adjusted for age, sex, scanner, and intracranial volume effects.  $d = .2$  indicates a small effect,  $d = .5$  a medium effect, and  $d \geq .8$  a large effect.<sup>27</sup> Note the different spectral results of the two modalities. The EEG connectivity increases in patients were significant in the delta, theta, and alpha frequencies with a centrottemporal focus. In the MEG analysis, the increases were most pronounced in the beta1 frequency and frontotemporal areas, but reached significance in all frequency bands studied (not shown). (C) The statistical combination of EEG and MEG patterns highlighted connectivity increases, particularly in the theta and beta frequency band. (D) Inclusion of cortical thickness in the joint analysis of EEG and MEG patterns resulted in more pronounced differences between patients and controls, especially in theta and beta1 frequencies and in frontal areas in other frequency bands. We used a nonparametric combination of EEG/MEG connectivity and cortical thickness based on Fisher's method,<sup>25</sup> with age, sex, scanner, and intracranial volume as covariates of no interest. FWE, familywise error; HD, high-density; MRI, magnetic resonance imaging



**(A) HD-EEG connectivity (GGE > controls)****(B) MEG connectivity (GGE > controls)****(C) Joint inference: connectivity HD-EEG + MEG (GGE > controls)****(D) Joint inference: connectivity + cortical thickness (HD-EEG + MEG + MRI)**

regions of the Desikan–Killiany atlas<sup>28</sup> and investigated separate regional group differences using PALM.

### 3 | RESULTS

#### 3.1 | Connectivity in GGE and siblings

Patients with GGE had higher connectivity than controls, reaching significance in lower frequencies in the vertex and global EEG analysis (delta, theta, and alpha frequency bands; Figure 2, Table S3). The EEG connectivity increases in patients were most pronounced in centrotemporal brain areas, whereas increases in the MEG analysis tended to have a frontotemporal focus across the entire frequency spectrum (Figure 1A,B). In the joint EEG and MEG vertex analysis, the increases were strongest in theta and beta1 but also included significant patterns in the delta and alpha frequencies (Figure 1C). When combining global EEG and MEG statistics, connectivity levels in patients were significantly higher than in controls in all frequency bands studied (Table S3).

Patients did not significantly differ from siblings, but siblings tended to have higher EEG connectivity than the patients in the beta2 and gamma frequency bands (vertex level and globally; Figure 2A, Table S3). In siblings, there was also a trend toward higher EEG connectivity compared with controls across the spectrum, but predominantly in the theta band without reaching significance (vertex level and globally; Figure 2A, Table S3). See Figure S1 for effect sizes of the differences between siblings and the other groups at the vertex level. In the MEG analysis, siblings showed higher connectivity than controls in the beta1 band, but also did not differ significantly from either the controls or the patients (vertex analysis not shown, global analysis in Table S3). Combining EEG and MEG statistics did not substantially change the findings of the separate analyses in siblings.

#### 3.2 | Power in GGE and siblings

EEG power was significantly higher in patients with GGE than in controls in all frequency bands studied (delta to gamma bands at vertex level and globally; Figure 4, Table S3). A posterior focus of power increases was observed in both EEG and MEG analyses, but especially for the MEG-derived patterns in all frequency bands (Figure 3A,B). In the joint EEG/MEG analysis, the power increases were most pronounced in posterior regions of the brain, that is, in occipital, temporoparietal, and central regions (delta to gamma bands; Figure 3C).

Patients with GGE also had higher power than their siblings, but to a lesser extent than controls. This increased

power was significant in the lower EEG frequency bands (delta and alpha at vertex level and globally; Figure 4A,C, Table S3) in the temporoposterior regions. In the MEG analysis, power was significantly increased occipitally and in all frequency bands except theta (not shown). In the joint vertex analyses, the power increases in patients compared with siblings were significant at all frequencies and at a global level in delta, alpha, and gamma (Table S3). There were no significant EEG power differences between siblings and controls, but standardized effect sizes indicated generally higher power in siblings than in controls (Figure S1). Similarly, MEG analysis revealed higher theta and beta power in siblings (vertex analysis not shown, global analysis in Table S3). Combining EEG and MEG statistics did not reveal notable changes compared with separate power analyses in siblings.

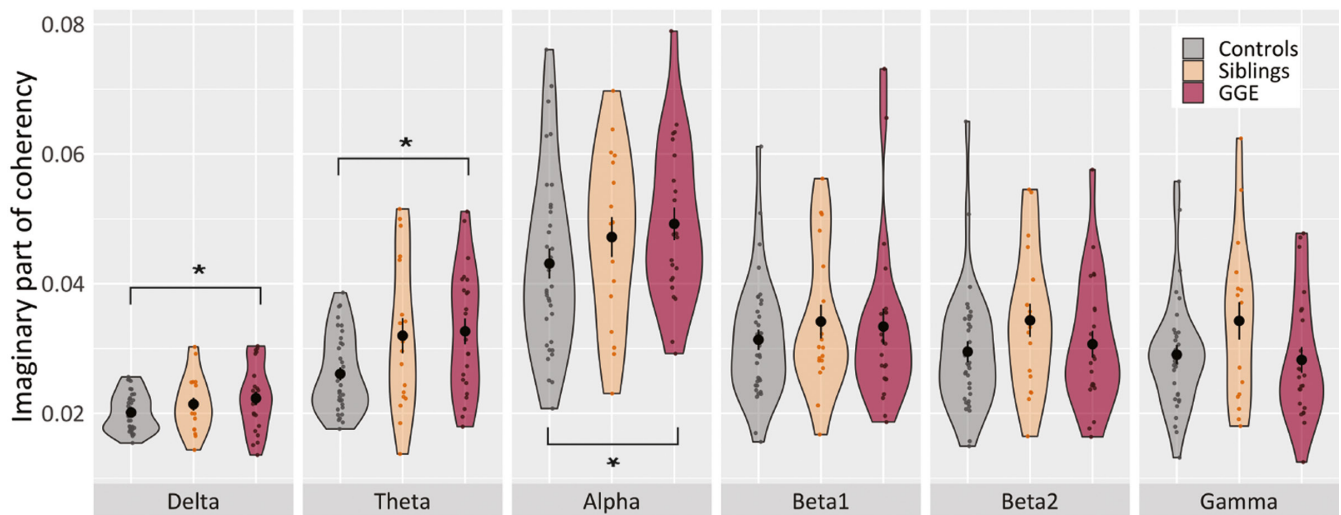
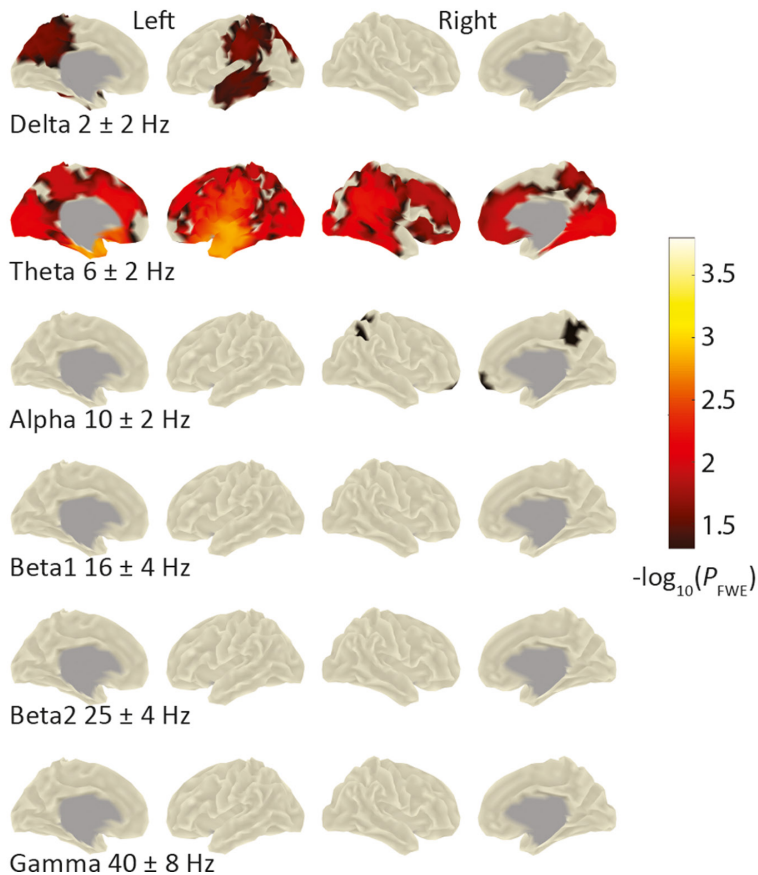
#### 3.3 | Joint inference of functional and structural metrics

The inclusion of cortical thickness in the joint connectivity analysis increased the statistical significance of group differences between patients and controls. This was particularly the case for the theta band in frontocentral and temporal regions (Figure 1D), with an average decrease of significant  $p$ -values by three  $-\log_{10}$  levels (Figure 5A). Probability values were also lower for the delta, alpha, and beta1 contrast (differences of 2–2.5  $-\log_{10}$  levels). In higher frequency bands, the group contrasts became mainly stronger in superior frontal regions (beta2, gamma; difference of  $\sim 1.5$   $-\log_{10}$  levels).

Power contrasts became stronger in all frequency bands and in occipitoparietal and central areas of the brain (Figures 3D and 5A; differences of  $\sim 4$   $-\log_{10}$  levels). Group comparisons between siblings and controls or patients and siblings did not change significantly when cortical thickness was taken into account.

#### 3.4 | Cortical thickness in GGE and siblings

Separate analyses in patients, siblings, and controls did not reveal significant group differences (at vertex level and globally,  $p > .05$ ). Regional standardized group mean differences, however, suggest cortical thinning in patients (Figure 5B) predominantly in the right hemisphere and paracentral and precentral gyri ( $d > .5$ ), and in frontoparietal regions and cuneus ( $d > .4$ ). These patterns were significant only in the uncorrected maps ( $p_{\text{uncorr}} < .05$ ). Siblings had lower cortical thickness than controls in frontocentral regions ( $d > .3$ ; Figure 5B). In the right supramarginal gyrus, right temporal

**(A) Global connectivity (HD-EEG)****(B) Connectivity GGE > controls**

**FIGURE 2** Electroencephalography (EEG) analyses of global and vertex connectivity. (A) Individual global connectivity values (imaginary part of coherency) of controls, siblings, and patients with genetic generalized epilepsy (GGE). Shown are the density of data, group means, and standard errors of means. Statistically significant group differences are marked with an asterisk ( $*p < .05$ ). See Table S2 for detailed results. (B) Significantly increased vertex connectivity is highlighted in patients compared with controls at a  $-\log_{10}p$  threshold of 1.3 (equivalent to  $p < .05$ ). The statistical comparisons at the vertex level between patients with GGE and their siblings and between siblings and controls did not yield significant results and are not shown. We used permutation-based analysis of linear models for global and vertex analyses with age, sex, scanner, and intracranial volume as covariates of no interest. Probability values were familywise error (FWE) corrected for whole-brain analyses within each frequency band and across the three modalities tested in this study (EEG, magnetoencephalography, and magnetic resonance imaging). HD, high-density



gyri, and left medial orbitofrontal regions, the siblings had a greater cortical thickness than controls ( $d > .4$ ), but the patterns did not survive corrections for multiple comparisons and were not present in the patients.

### 3.5 | Clinical factors

To assess whether the intake of medication influenced the structural and functional metrics, we split the patient group according to antiepileptic drug exposure. Functional connectivity was generally lower in patients taking two or more drugs ( $n = 6$ ) than in patients taking none or one drug ( $n = 17$ ). This finding was observed using both EEG and MEG, and was significant in the beta1 band of vertex-level analyses (single and joint inference; [Figure 6B](#)) and global analyses (global EEG:  $t_{17} = -1.94$ ,  $p = .039$ ,  $d = -.94$ ; MEG:  $t_{17} = -1.83$ ,  $p = .046$ ,  $d = -.89$ ; joint inference  $p = .015$ ). The global EEG connectivity mean of the patients with high drug exposure was also lower than the mean of the controls and siblings (mainly in the delta, beta1, beta2, and gamma bands; [Figure 6A](#)), which was not the case in the MEG analysis (not shown). Neither EEG nor MEG power of the patients differed significantly with respect to drug exposure (vertex level and globally,  $p > .05$ ). Cortical thickness did not differ in relation to antiepileptic drug exposure (vertex level and globally,  $p > .05$ ).

The assessment of other clinical variables (occurrence of GSWD during EEG/MEG recordings, seizure control) was complicated by the small sample sizes, unequal sex ratios, and age distributions in the patient subgroups. Because EEG power differed between sexes and cortical thickness varied with age, we were unable to distinguish these effects from the effects of interest.

## 4 | DISCUSSION

We combined electrophysiological signals at rest and cortical morphology to advance our understanding of network pathology in GGE and its genetic basis. EEG detected functional alterations similar to MEG, but with

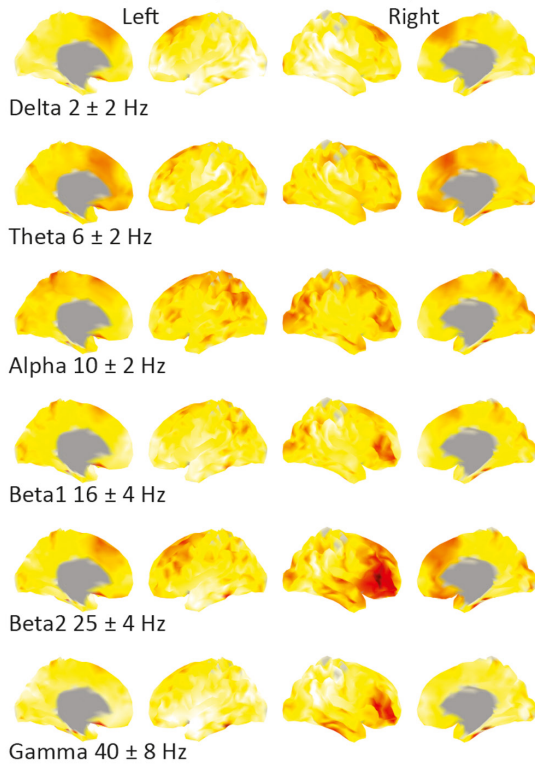
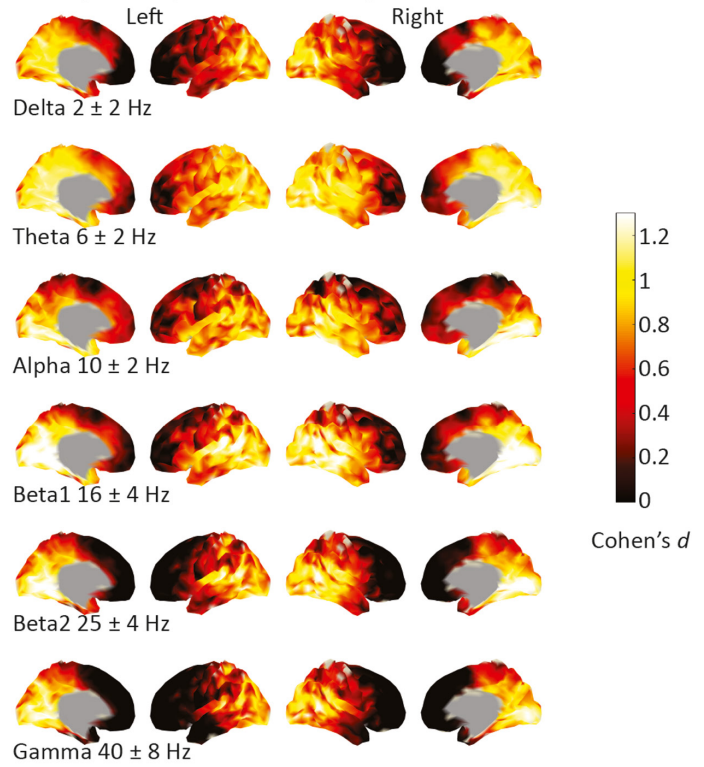
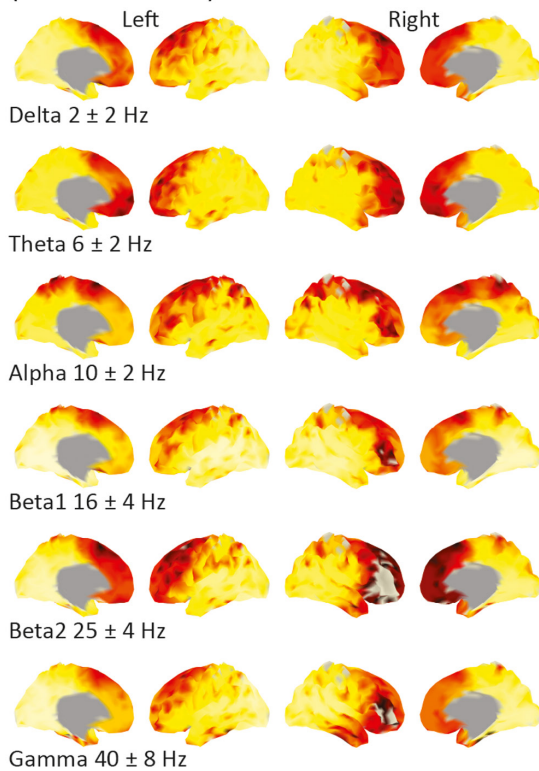
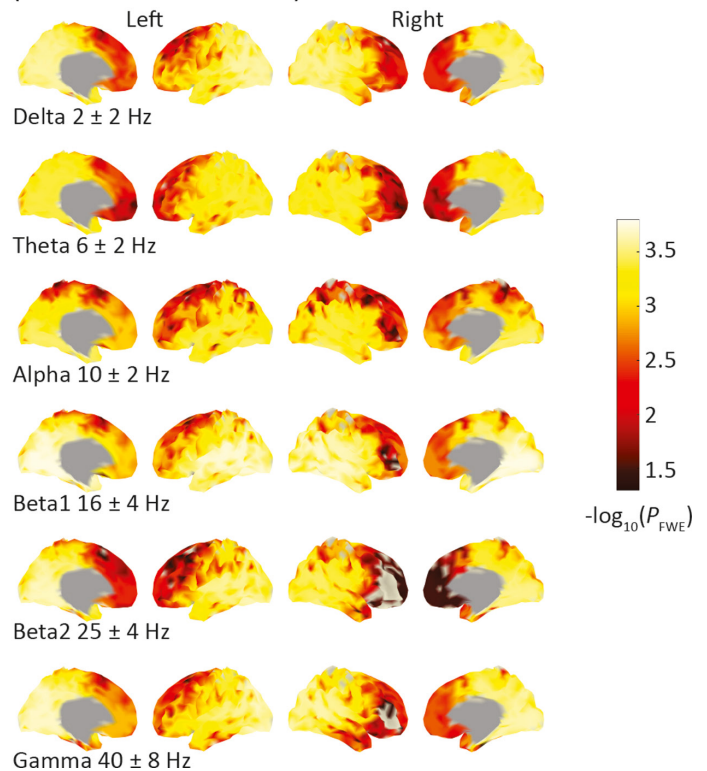
a different spectral sensitivity profile. The statistical integration of both modalities suggests a significant role of theta and beta oscillations in GGE. Cortical thinning was observed in our GGE cohort and amplified the functional group contrast when jointly analyzed. Similar functional and structural characteristics in healthy siblings of the patients suggest genetic contribution to the imaging patterns.

Aberrant neuronal excitability and synchronization during the ictal state typically play a crucial role in epilepsy.<sup>29</sup> Even in the interictal state, patients with GGE have higher global and large-scale synchronization and power, as observed using EEG and MEG with spectral differences relevant for comparisons of clinical studies. The joint EEG/MEG analysis revealed significant connectivity increases in the delta to beta1 frequency bands, with a broader spectral distribution in MEG, peaking in the beta1 band, as previously described in this<sup>2</sup> and other cohorts.<sup>30,31</sup> Conversely, EEG was more sensitive to increases in the lower frequencies, particularly in theta. This could have several reasons. In line with previous studies, high drug exposure likely had a normalizing effect<sup>32</sup> that was significant for the EEG beta1 band and less pronounced in the MEG analysis. It is also possible that the phase estimation in the higher EEG frequencies was noisier than with MEG, despite careful artifact suppression, possibly due to greater susceptibility to electromyogenic effects.<sup>33,34</sup> While studies on electrophysiological connectivity in GGE are still limited, more is known about oscillatory power in this condition. Most resting state EEG studies have associated GGE with power increases in the theta frequency band, followed by increases in the beta band, with mixed results for other frequencies.<sup>35</sup> However, the choice of channel density, analysis space, and patient characteristics has been inconsistent across studies and presents a challenge to the comparability of results.<sup>35</sup> We used EEG and MEG systems with comparable channel coverage and analysis pipelines in the same individuals and observed increased power in both modalities and across the conventional frequency spectrum.

Genetic generalized epilepsy phenotypes within each modality were spatially similar across the

**FIGURE 3** Effect sizes of electroencephalography (EEG) and magnetoencephalography (MEG) power increases in genetic generalized epilepsy (GGE), and joint inference with and without cortical thickness. (A, B) Standardized effect sizes (Cohen  $d$ ) for increased power in patients with GGE versus controls using EEG and MEG, respectively. Effect sizes were derived from the  $t$ -values of the permutation analyses of linear models.  $d$  is therefore adjusted for age, sex, scanner, and intracranial volume effects.  $d = .2$  indicates a small effect,  $d = .5$  a medium effect, and  $d \geq .8$  a large effect.<sup>27</sup> The power increases in GGE patients were significant across the frequency spectrum, with a stronger posterior focus in MEG compared with EEG. (C) The power increases in the joint analysis of EEG and MEG were prominent in the occipital and temporoparietal regions. (D) The inclusion of cortical thickness in the joint analysis of EEG and MEG patterns resulted in more pronounced power differences between patients and controls in temporoparietal regions. We used a nonparametric combination of EEG/MEG connectivity and cortical thickness based on Fisher's method,<sup>25</sup> with age, sex, scanner, and intracranial volume as covariates of no interest. FWE, familywise error; HD, high-density; MRI, magnetic resonance imaging

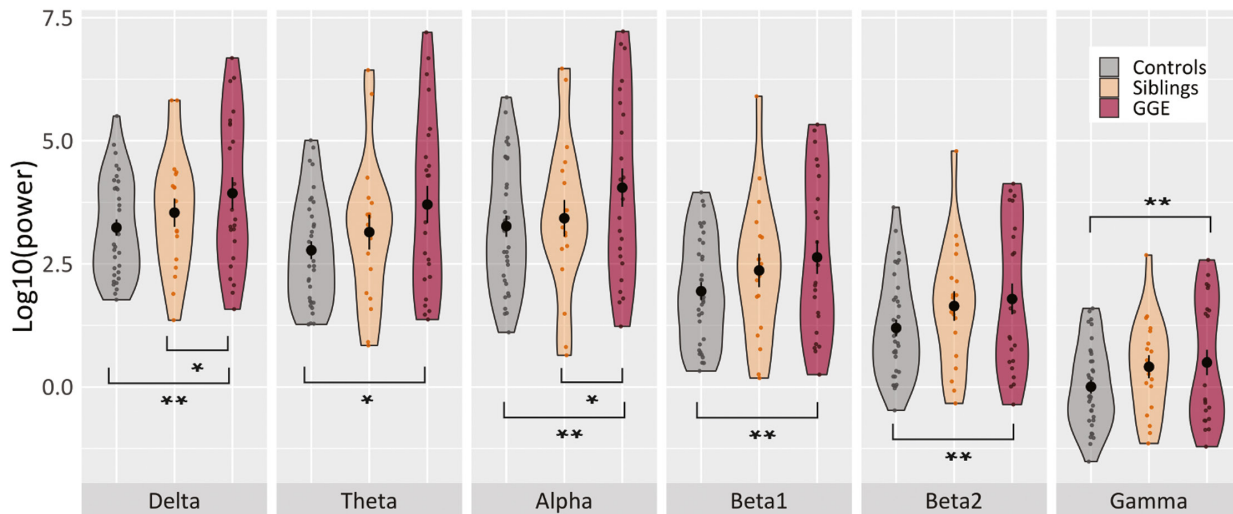


**(A) HD-EEG power (GGE > controls)****(B) MEG power (GGE > controls)****(C) Joint inference: power HD-EEG + MEG (GGE > controls)****(D) Joint inference: power + cortical thickness (HD-EEG + MEG + MRI)**

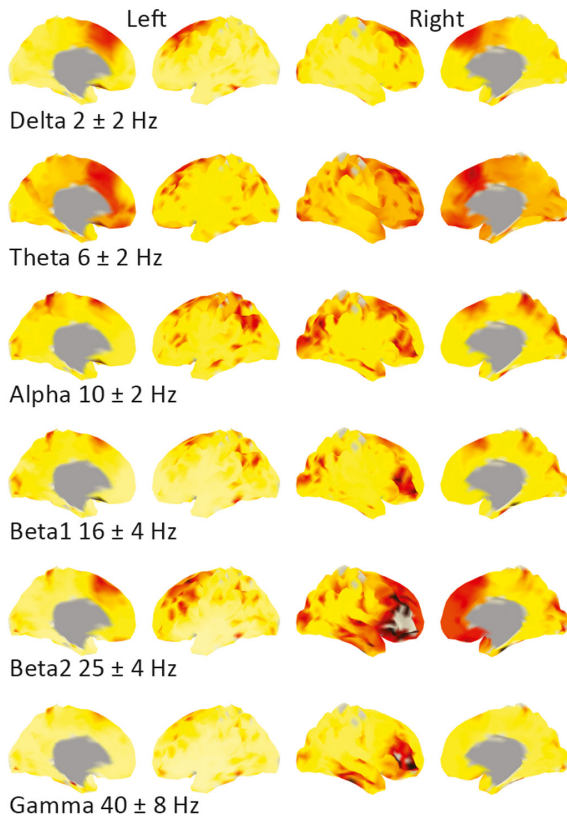
frequency spectrum. This is consistent with the idea of a timescale-invariant spatial organization of the electrophysiological connectome<sup>36</sup>; that is, neuronal signals

likely operate within the same networks at different timescales. It is conceivable that GGE-typical changes are reflected in the broadband and similar brain regions,

## (A) Global power (HD-EEG)



## (B) Power GGE &gt; controls



## (C) Power GGE &gt; siblings

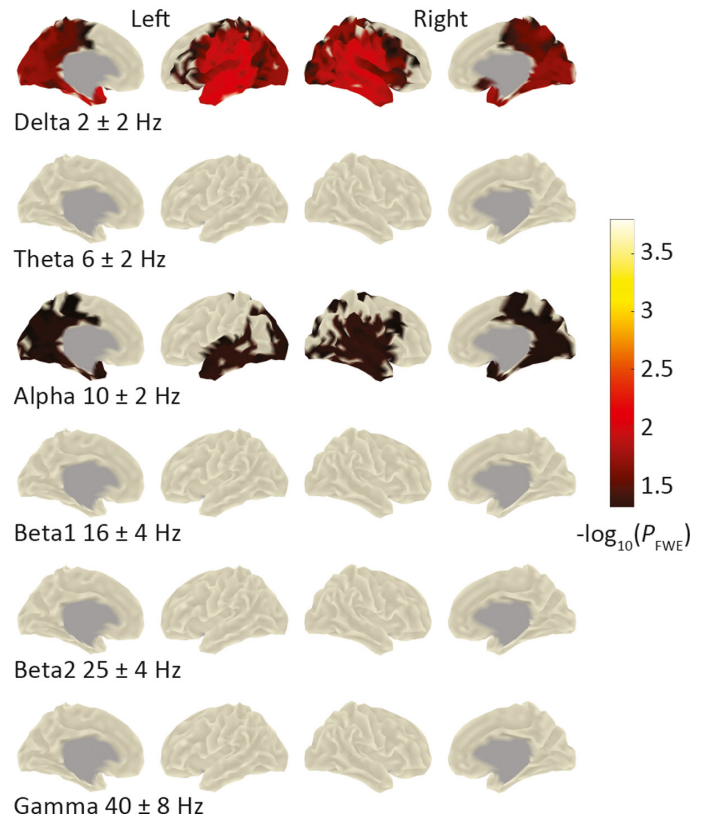


**FIGURE 4** Electroencephalographic (EEG) analyses of global and vertex power. (A) Individual global power values of controls, siblings, and patients with genetic generalized epilepsy (GGE). Shown are the density of data, group means, and standard errors of means. Statistically significant group differences are marked with asterisks (\* $p < .05$ , \*\* $p < .001$ ). See Table S2 for more detailed results. (B, C) Significantly increased vertex power is highlighted in patients compared with controls, and in patients compared with siblings, respectively, at a  $-\log_{10}p$  threshold of 1.3 (equivalent to  $p < .05$ ). Differences in vertex power between siblings and controls were not significant and are not shown. We used permutation analysis of linear models for global and vertex analyses with age, sex, scanner, and intracranial volume as covariates of no interest. Probability values were familywise error (FWE) corrected for whole-brain analyses within each frequency band and across the three modalities tested in this study (EEG, magnetoencephalography, and magnetic resonance imaging). HD, high-density

with a dominant role of theta and beta oscillations particularly evident in our joint EEG/MEG analysis. Furthermore, the spatial representation of GGE patterns differed between the modalities. Frontotemporal connectivity alterations were more readily detected by MEG, whereas increased EEG connectivity was more pronounced in central regions. The power patterns were more widespread in the EEG analysis and focused on the posterior regions in the MEG analysis. This difference in focality may be due to distinct signal origins resulting in a clearer separation of cortical sources in MEG, as well as greater spatial smearing of electrical signals due to different tissue conductances.<sup>3</sup> Also, EEG tends to measure differently oriented sources and MEG captures mainly tangential currents originating in cortical fissures.<sup>37</sup> On the other hand, the signal-to-noise ratio varies depending on the modality, brain region, and frequency, which limits the comparability of the contrast maps. Also, we recorded EEG and MEG separately, and the choice of the head model and slightly different measurement conditions may have introduced a bias. Direct comparisons of simultaneously recorded MEG/EEG have shown that both methods measure the same intrinsic network,<sup>38</sup> especially between 8 and 32 Hz.<sup>39</sup> However, different spatial sensitivity for frontoparietal connections and effects of head model complexity were found.<sup>38</sup> To take advantage of both methods, we adopted a combined approach, which provided new insights into the network characteristics of GGE.

Moreover, we provide evidence for the heritability of EEG phenotypes. There was an intermediate position of network levels in siblings, except for beta and gamma connectivity. Here, the global mean in the siblings was higher than that in the patients, which may be partly related to medication effects in the patients as observed in the beta frequencies. For MEG phenotypes, we previously demonstrated that heritability was strongest in beta frequencies.<sup>2</sup> Altogether, we have extended previous endophenotype research in GGE and juvenile myoclonic epilepsy (JME)<sup>11–15</sup> by showing that resting state alterations measured at high temporal resolution cosegregate in families with affected members. In addition to genetic factors, environmental and/or acquired factors might also have contributed to the phenotypic similarity between the patients and siblings, which cannot be excluded in this study. However, consistent with the prerequisites for an endophenotype,<sup>10</sup> high power and synchrony previously correlated with disease activity such as GSWD,<sup>2</sup> which also occur in healthy siblings with a higher likelihood.<sup>40</sup> A recent genetic correlation study supports the notion of an endophenotype based on fast brain oscillations. Genetic risk for increased theta and beta power, as measured at the vertex (Cz)

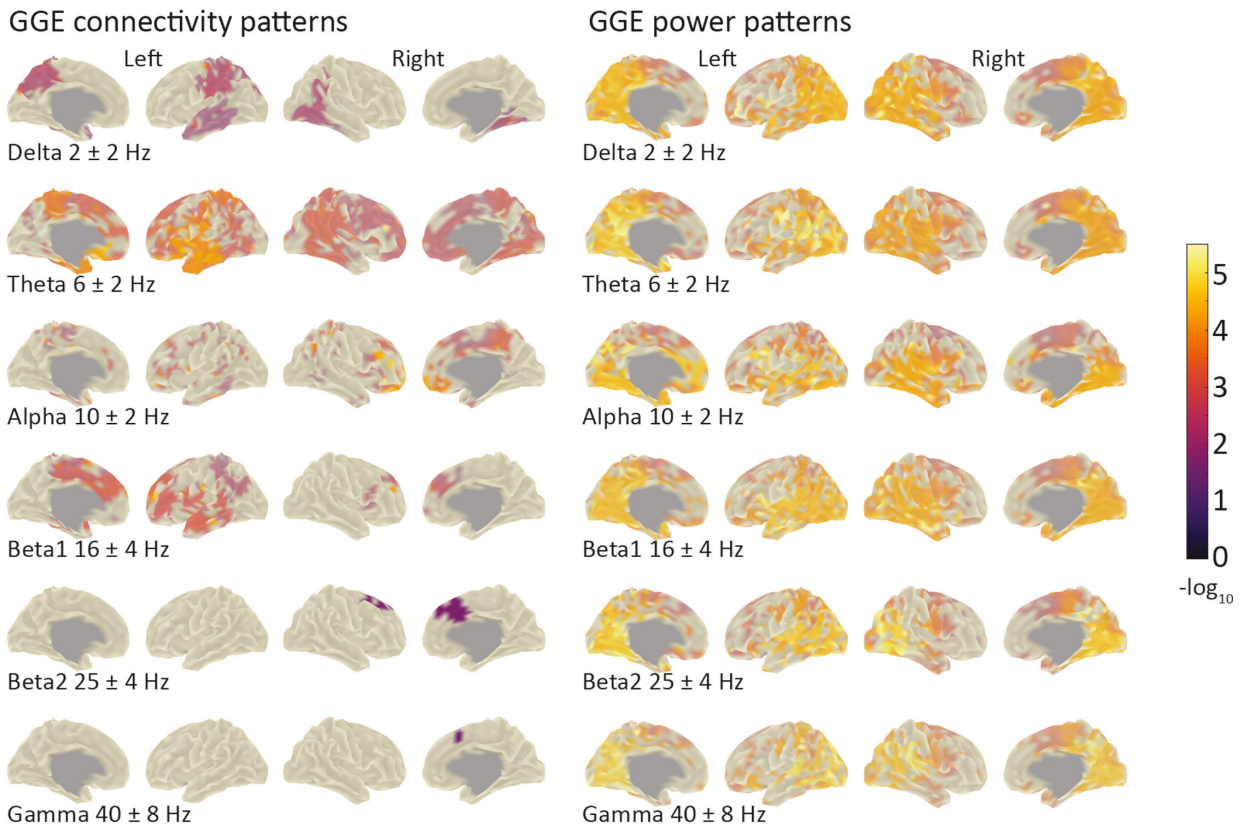
electrode, was associated with a higher risk for GGE.<sup>41</sup> Beta oscillations have been linked to motor control<sup>42</sup> and  $\gamma$ -aminobutyric acidergic mechanisms,<sup>43</sup> which in turn play a meaningful role in the pathology of GGE.<sup>44</sup> Theta rhythms are thought to be involved in hippocampal networks.<sup>45</sup> In animal models of temporal lobe epilepsy, increased theta synchronization in the transition phase to seizures<sup>46</sup> and coupling to the prefrontal cortex have been observed.<sup>47</sup>

When cortical thickness was added to the connectivity analyses, the differences between patients and controls were amplified, especially in the theta and beta bands, and anterior and central brain regions. Power contrasts in posterior regions were also strengthened, suggesting a relationship between aberrant morphology and functional organization in GGE. Clearly, this interplay requires further investigations. The spatial correspondence between functional MRI connectivity and cortical atrophy in GGE has been studied earlier, but without significant results.<sup>8</sup> We did not directly assess the structure–function relationship, but statistically combined multiple modalities, which can provide greater power than separate analyses.<sup>24</sup> Thus, it is easier to detect a true effect that acts on all measured characteristics simultaneously.<sup>24</sup> The separate analysis of cortical thickness revealed a reduction in patients with a central focus consistent with earlier findings,<sup>6,8</sup> but significance did not survive corrections for multiple testing. Nonetheless, the functional contrasts benefited from taking cortical thickness into account, which argues for the integration of the three modalities to improve diagnostic and prediction accuracy.<sup>48</sup> In addition, cortical thinning in GGE may not simply reflect disease activity but also genetic background. In our study, siblings without epilepsy also had reduced cortical thickness in the superior frontal and paracentral areas, arguing against a change subsequent to seizures and disease progression alone. A larger sample is needed to validate these results, but strong evidence for genetic risk signals enriched in the frontal cortex has also been demonstrated in a recent genome-wide mega-analysis.<sup>49</sup> Other markers such as altered curvature and surface area have been proposed as endophenotypes in JME,<sup>7</sup> but these likely underlie other neurodevelopmental trajectories.<sup>50</sup>

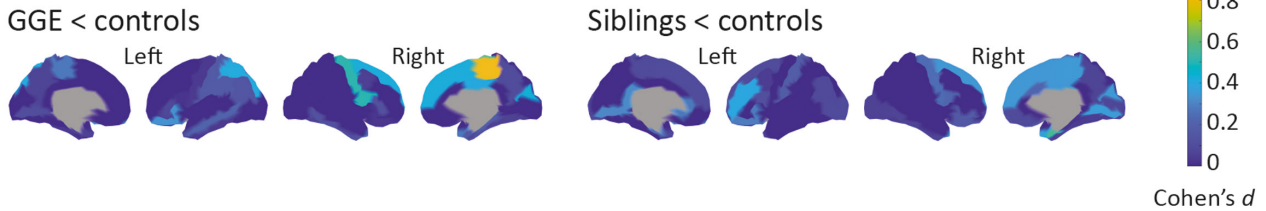
Overall, the integration of MEG and EEG resting state signatures and brain morphology provided valuable information concerning GGE pathophysiology. Our investigations in siblings without active epilepsy suggest that the observed imaging phenotypes are likely genetically driven. These findings pave the way to advance the deciphering of the genetic predisposition to GGE using imaging metrics.



**(A) Statistical increases of functional contrasts after inclusion of cortical thickness (*p*-value difference)**



**(B) Effect sizes for decreases in regional cortical thickness**



**(C) Individual cortical thickness for regions with decreases in GGE (Cohen's *d* > 0.4)**

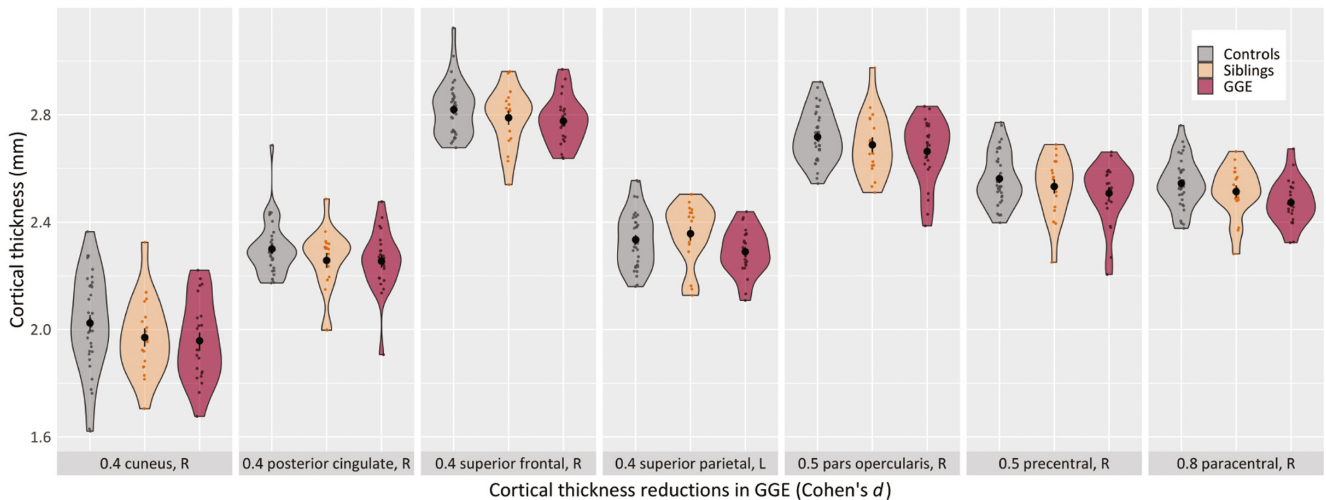
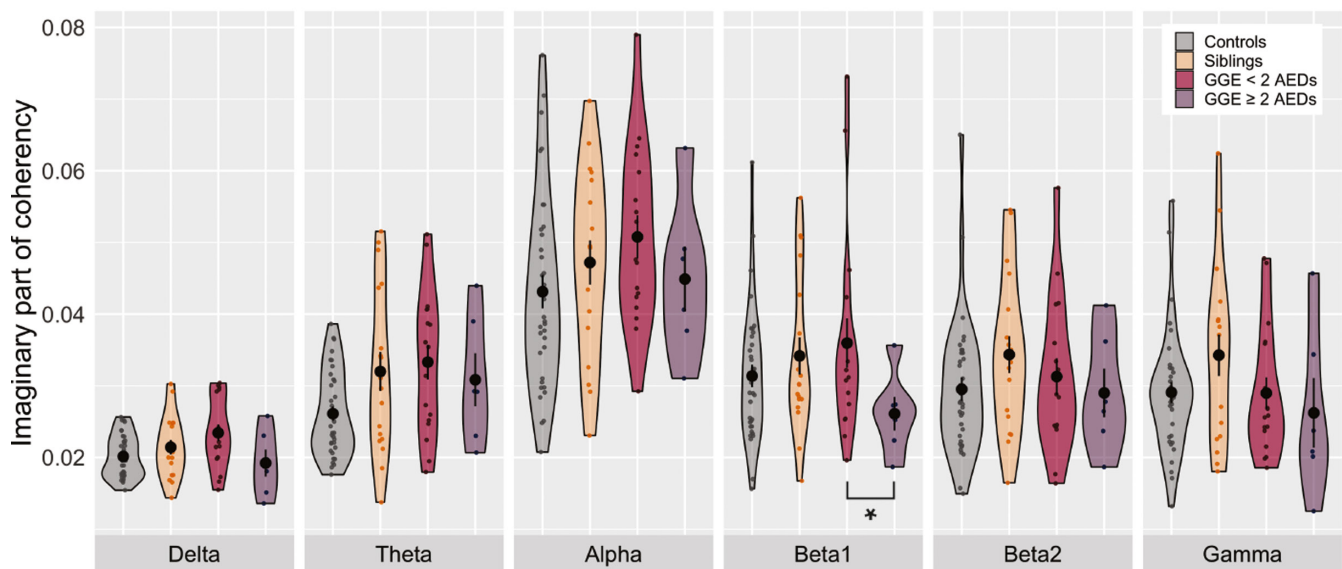




**FIGURE 5** Effects of cortical thickness on joint inference analysis and group-level differences. (A) When cortical thickness was jointly analyzed with functional data (electroencephalography + magnetoencephalography), the connectivity patterns of genetic generalized epilepsy (GGE) patients were amplified mainly in the theta and beta frequency bands. The power patterns became stronger in temporoparietal and occipital regions. The plot shows significant vertices with an increase in the  $p$ -value ( $-\log_{10}$  difference) after adding cortical thickness to the joint functional analysis. (B) The plot shows standardized effect sizes (Cohen  $d$ ) for reduced cortical thickness in patients with GGE against controls, and in siblings against controls, respectively. Effect sizes were derived from the  $t$ -values of the permutation analysis of linear models in cortical regions (Desikan–Killiany atlas).<sup>28</sup>  $d$  is therefore adjusted for age, sex, scanner, and intracranial volume effects.  $d = .2$  indicates a small effect,  $d = .5$  a medium effect, and  $d \geq .8$  a large effect.<sup>27</sup> (C) The violin plot shows individual thickness values for cortical regions, in which patients with GGE had lower cortical thickness than controls (Cohen  $d > .4$ ). Individual cortical thickness values were adjusted for effects of age, sex, scanner, and total intracranial volume. L, left; R, right

### (A) Global HD-EEG connectivity and AED exposure



### (B) Joint inference HD-EEG + MEG (low load > high load AEDs)

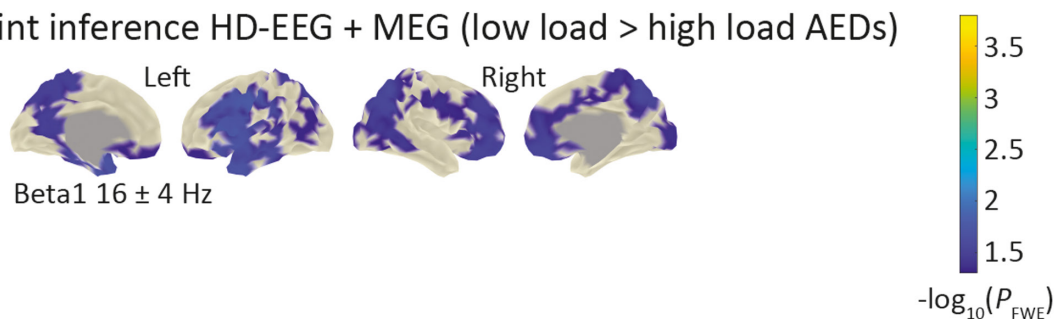


**FIGURE 6** Antiepileptic medication and decreased connectivity in genetic generalized epilepsy (GGE). (A) Individual global connectivity for separate electroencephalographic (EEG) analyses in controls, siblings, and patients with low ( $n = 17$ ) and high drug load ( $n = 6$ ). The violin plots show the density of data, group means, and standard errors of means. Statistically significant differences between the patient subgroups are marked with an asterisk ( $*p < .05$ ). See Figure 2A for significant connectivity differences between the main groups (controls, siblings, and patients). Global and (B) vertex connectivity was significantly lower in patients taking two or more antiepileptic drugs (AEDs; high load) at the time of the measurement than in patients taking fewer than two drugs (low load). This effect was observed in separate EEG and magnetoencephalography (MEG) analyses as well as in the joint analysis, but was more pronounced in EEG than in MEG. Vertices are color-coded at a  $-\log_{10}p$  threshold of 1.3 (equivalent to  $p < .05$  familywise error [FWE] corrected). Results for global and vertex analyses were obtained by permutation testing of linear models with age, sex, scanner, and intracranial volume as covariates of no interest. HD, high-density

## ACKNOWLEDGMENTS

This work was supported by the German Research Foundation (FO 750/5-1 to N.K.F.). We would like to express our gratitude to the patients, their families, and control individuals for study participation. We thank Sangyeob Baek, Silvia Vannoni, and Dr Silke Klamer-Ethofer for their assistance with data acquisition. We are grateful to Prof Dr Yvonne Weber for the provision of clinical information.

## CONFLICT OF INTEREST

N.K.F. has received honoraria from Arvelle, Bial, Eisai, and EGI-Phillips, all unrelated to the current work. J.M. has received lecture fees and travel support from UCB, Eisai, Desitin, Alexion, GW-Pharma, and the German Society for Ultrasound, all unrelated to the current study. H.L. has received speaker bureau and consultancy fees from Arvelle, Bial, BioMarin, Eisai, and UCB, all unrelated to this study. None of the other authors has any conflict of interest to disclose. We confirm that we have read the Journal's position on issues involved in ethical publication and affirm that this report is consistent with those guidelines.

## ORCID

Christina Stier  <https://orcid.org/0000-0001-5707-4885>

Niels K. Focke  <https://orcid.org/0000-0001-5486-6289>

## REFERENCES

- Koeleman BP. What do genetic studies tell us about the heritable basis of common epilepsy? Polygenic or complex epilepsy? *Neurosci Lett*. 2018;667:10–6.
- Stier C, Elshahabi A, Hegner YL, Kotikalapudi R, Marquetand J, Braun C, et al. Heritability of magnetoencephalography phenotypes among patients with genetic generalized epilepsy and their siblings. *Neurology*. 2021;97:e166–77.
- daSilva FL. EEG and MEG: relevance to neuroscience. *Neuron*. 2013;80:1112–28.
- Heers M, Rampp S, Kaltenhäuser M, Pauli E, Rauch C, Dölken MT, et al. Detection of epileptic spikes by magnetoencephalography and electroencephalography after sleep deprivation. *Seizure*. 2010;19:397–403.
- Stefan H, Paulini-Ruf A, Hopfengärtner R, Rampp S. Network characteristics of idiopathic generalized epilepsies in combined MEG/EEG. *Epilepsy Res*. 2009;85:187–98.
- Whelan CD, Altmann A, Botía JA, Jahanshad N, Hibar DP, Absil J, et al. Structural brain abnormalities in the common epilepsies assessed in a worldwide ENIGMA study. *Brain*. 2018;141:391–408.
- Wandschneider B, Hong S-J, Bernhardt BC, Fadaie F, Vollmar C, Koepf MJ, et al. Developmental MRI markers cosegregate juvenile patients with myoclonic epilepsy and their healthy siblings. *Neurology*. 2019;93:e1272–80.
- Larivière S, Rodríguez-Cruces R, Royer J, Caligiuri ME, Gambardella A, Concha L, et al. Network-based atrophy modeling in the common epilepsies: a worldwide ENIGMA study. *Sci Adv*. 2020;6:eabc6457.
- Panizzon MS, Fennema-Notestine C, Eyer LT, Jernigan TL, Prom-Wormley E, Neale M, et al. Distinct genetic influences on cortical surface area and cortical thickness. *Cereb Cortex*. 2009;19:2728–35.
- Gottesman II, Gould TD. The endophenotype concept in psychiatry: etymology and strategic intentions. *Am J Psychiatry*. 2003;160:636–45.
- Caciagli L, Wandschneider B, Xiao F, Vollmar C, Centeno M, Vos SB, et al. Abnormal hippocampal structure and function in juvenile myoclonic epilepsy and unaffected siblings. *Brain*. 2019;142:2670–87.
- Wandschneider B, Centeno M, Vollmar C, Symms M, Thompson PJ, Duncan JS, et al. Motor co-activation in siblings of patients with juvenile myoclonic epilepsy: an imaging endophenotype? *Brain*. 2014;137:2469–79.
- Caciagli L, Wandschneider B, Centeno M, Vollmar C, Vos SB, Trimmel K, et al. Motor hyperactivation during cognitive tasks: an endophenotype of juvenile myoclonic epilepsy. *Epilepsia*. 2020;61:1438–52.
- Vollmar C, O'Muircheartaigh J, Barker GJ, Symms MR, Thompson P, Kumari V, et al. Motor system hyperconnectivity in juvenile myoclonic epilepsy: a cognitive functional magnetic resonance imaging study. *Brain*. 2011;134:1710–9.
- Tangwiriyaikul C, Perani S, Abela E, Carmichael DW, Richardson MP. Sensorimotor network hypersynchrony as an endophenotype in families with genetic generalized epilepsy: a resting-state functional magnetic resonance imaging study. *Epilepsia*. 2019;60:e14–9.
- Chowdhury FA, Woldman W, FitzGerald TH, Elwes RDC, Nashef L, Terry JR, et al. Revealing a brain network endophenotype in families with idiopathic generalised epilepsy. *PLoS One*. 2014;9:e110136.
- Scheffer IE, Berkovic S, Capovilla G, Connolly MB, French J, Guilhoto L, et al. ILAE classification of the epilepsies: position paper of the ILAE Commission for Classification and Terminology. *Epilepsia*. 2017;58:512–21.
- Saad ZS, Reynolds RC. SUMA. *NeuroImage*. 2012;62:768–73.
- Oostenveld R, Fries P, Maris E, Schoffelen J-M. FieldTrip: open source software for advanced analysis of MEG, EEG, and invasive electrophysiological data. *Comput Intellig Neurosci*. 2011;2011:1–9.
- Marquetand J, Vannoni S, Carboni M, Li Hegner Y, Stier C, Braun C, et al. Reliability of magnetoencephalography and high-density electroencephalography resting-state functional connectivity metrics. *Brain Connect*. 2019;9:539–53.
- Gross J, Kujala J, Hämäläinen M, Timmermann L, Schnitzler A, Salmelin R. Dynamic imaging of coherent sources: studying neural interactions in the human brain. *Proc Natl Acad Sci U S A*. 2001;98:694–9.
- Nolte G, Bai O, Wheaton L, Mari Z, Vorbach S, Hallett M. Identifying true brain interaction from EEG data using the imaginary part of coherency. *Clin Neurophysiol*. 2004;115:2292–307.
- Chung MK. Heat kernel smoothing and its application to cortical manifolds. Technical report. Madison, WI: Department of Statistics, University of Wisconsin-Madison; 2004.
- Winkler AM, Webster MA, Brooks JC, Tracey I, Smith SM, Nichols TE. Non-parametric combination and related permutation tests for neuroimaging. *Hum Brain Mapp*. 2016;37:1486–511.

25. Fisher R. *Statistical methods for research workers*. 4th ed. Edinburgh, UK: Edition Oliver & Boyd; 1932.
26. Smith SM, Nichols TE. Threshold-free cluster enhancement: addressing problems of smoothing, threshold dependence and localisation in cluster inference. *NeuroImage*. 2009;44:83–98.
27. Cohen J. A power primer. *Psychol Bull*. 1992;112:155.
28. Desikan RS, Ségonne F, Fischl B, Quinn BT, Dickerson BC, Blacker D, et al. An automated labeling system for subdividing the human cerebral cortex on MRI scans into gyral based regions of interest. *NeuroImage*. 2006;31:968–80.
29. Jiruska P, De Curtis M, Jefferys JG, Schevon CA, Schiff SJ, Schindler K. Synchronization and desynchronization in epilepsy: controversies and hypotheses. *J Physiol*. 2013;591:787–97.
30. Li Hegner Y, Marquetand J, Elshahabi A, Klamer S, Lerche H, Braun C, et al. Increased functional MEG connectivity as a hallmark of MRI-negative focal and generalized epilepsy. *Brain Topogr*. 2018;31:863–74.
31. Elshahabi A, Klamer S, Sahib AK, Lerche H, Braun C, Focke NK. Magnetoencephalography reveals a widespread increase in network connectivity in idiopathic/genetic generalized epilepsy. *PLoS One*. 2015;10:e0138119.
32. Clemens B, Piros P, Bessenyi M, Hollódy K. Lamotrigine decreases EEG synchronization in a use-dependent manner in patients with idiopathic generalized epilepsy. *Clin Neurophysiol*. 2007;118:910–7.
33. Muthukumaraswamy S. High-frequency brain activity and muscle artifacts in MEG/EEG: a review and recommendations. *Front Hum Neurosci*. 2013;7:138.
34. Claus S, Velis D, daSilva FHL, Viergever MA, Kalitzin S. High frequency spectral components after secobarbital: the contribution of muscular origin—a study with MEG/EEG. *Epilepsy Res*. 2012;100:132–41.
35. Faiman I, Smith S, Hodsoll J, Young AH, Shotbolt P. Resting-state EEG for the diagnosis of idiopathic epilepsy and psychogenic nonepileptic seizures: a systematic review. *Epilepsy Behav*. 2021;121:108047.
36. Mostame P, Sadaghiani S. Oscillation-based connectivity architecture is dominated by an intrinsic spatial organization, not cognitive state or frequency. *J Neurosci*. 2021;41:179–92.
37. Hari R, Puce A. *MEG-EEG primer*. Oxford, UK: Oxford University Press; 2017.
38. Coquelet N, De Tiège X, Destoky F, Roshchupkina L, Bourguignon M, Goldman S, et al. Comparing MEG and high-density EEG for intrinsic functional connectivity mapping. *NeuroImage*. 2020;210:116556.
39. Siems M, Pape A-A, Hipp JF, Siegel M. Measuring the cortical correlation structure of spontaneous oscillatory activity with EEG and MEG. *NeuroImage*. 2016;129:345–55.
40. Tashkandi M, Baarma D, Tricco AC, Boelman C, Alkhatir R, Minassian BA. EEG of asymptomatic first-degree relatives of patients with juvenile myoclonic, childhood absence and rolandic epilepsy: a systematic review and meta-analysis. *Epileptic Disord*. 2019;21:30–41.
41. Stevelink R, Luykx JJ, Lin BD, Leu C, Lal D, Smith AW, et al. Shared genetic basis between genetic generalized epilepsy and background electroencephalographic oscillations. *Epilepsia*. 2021;62:1518–27.
42. Engel AK, Fries P. Beta-band oscillations—signalling the status quo? *Curr Opin Neurobiol*. 2010;20:156–65.
43. Baumgarten TJ, Oeltzschner G, Hoogenboom N, Wittsack H-J, Schnitzler A, Lange J. Beta peak frequencies at rest correlate with endogenous GABA+/Cr concentrations in sensorimotor cortex areas. *PLoS One*. 2016;11:e0156829.
44. May P, Girard S, Harrer M, Bobbili DR, Schubert J, Wolking S, et al. Rare coding variants in genes encoding GABAA receptors in genetic generalised epilepsies: an exome-based case-control study. *Lancet Neurol*. 2018;17:699–708.
45. Colgin LL. Rhythms of the hippocampal network. *Nat Rev Neurosci*. 2016;17:239–49.
46. Moxon KA, Shahlaie K, Girgis F, Saez I, Kennedy J, Gurkoff GG. From adagio to allegretto: the changing tempo of theta frequencies in epilepsy and its relation to interneuron function. *Neurobiol Dis*. 2019;129:169–81.
47. Broggin ACS, Esteves IM, Romcy-Pereira RN, Leite JP, Leao RN. Pre-ictal increase in theta synchrony between the hippocampus and prefrontal cortex in a rat model of temporal lobe epilepsy. *Exp Neurol*. 2016;279:232–42.
48. Abbasi B, Goldenholz DM. Machine learning applications in epilepsy. *Epilepsia*. 2019;60:2037–47.
49. International League Against Epilepsy Consortium on Complex Epilepsies. Genome-wide mega-analysis identifies 16 loci and highlights diverse biological mechanisms in the common epilepsies. *Nat Commun* 2018;9:5269.
50. Chen C-H, Fiecas M, Gutiérrez E, Panizzon MS, Eyler LT, Vuoksimaa E, et al. Genetic topography of brain morphology. *Proc Natl Acad Sci U S A*. 2013;110:17089–94.

## SUPPORTING INFORMATION

Additional supporting information may be found in the online version of the article at the publisher's website.

**How to cite this article:** Stier C, Loose M, Kotikalapudi R, Elshahabi A, Li Hegner Y, Marquetand J, et al. Combined electrophysiological and morphological phenotypes in patients with genetic generalized epilepsy and their healthy siblings. *Epilepsia*. 2022;63:1643–1657. <https://doi.org/10.1111/epi.17258>